JOURNAL OF SPACECRAFT AND ROCKETS
Vol. 41, No. 2, March–April 2004

2002 Version of the Aeroprediction Code (AP02)

F. G. Moore*
Aeroprediction, Inc., King George, Virginia 22485
and
T. C. Hymer†
U.S. Naval Surface Warfare Center, Dahlgren, Virginia 22448

The 2002 Version of the Aeroprediction Code (AP02) has been developed to address the requirements arising from advanced weapon concepts. The AP02 was formed by adding significant new technology and several productivity improvements to the 1993 Version of the Aeroprediction Code (AP93). New technology added included six- and eight- fin aerodynamics, improved nonlinear aerodynamics, improved pitch damping predictions, improved power-on-base drag estimates, base-bleed effect on base drag estimation, improved axial force of nonaxisymmetric bodies, and trailing-edge flap capability. Other improvements and productivity enhancements include an aerodynamic smoother, ballistic, and three-degree-of-freedom simulation modules, as well as refinements for the pre- and postprocessor for inputs and outputs of the AP02. Comparison of the predicted aerodynamics of the AP02 to AP98 and experimental data showed the AP02 to be slightly better than the AP98 in most cases that both codes would handle. However, due to the additional new technology incorporated into the AP02, many new options are available in the AP02 that are not available in the AP98. Therefore, the AP02 is more robust and, on average, is slightly more accurate than the AP98 in predicting aerodynamics of weapons.

Nomenclature

A_j, A_t = area of rocket motor nozzle exit and throat cross section, respectively, ft^2
A_{ref} = reference area (maximum cross-sectional area of body, if a body is present, or planform area of wing, if wing alone), ft^2
a, b = semimajor and semiminor axis, respectively, of ellipse, ft
C_A = axial-force coefficient
C_{A_B}, C_{A_F}, C_{A_W} = base, skin-friction, and wave components, respectively, of axial force coefficient
$C_{A_{\text{SF}}}$ = axial-force coefficient of a single fin
C_D = drag coefficient
cir = circumference of body, ft
C_M = pitching moment coefficient (based on reference area and body diameter, if body present, or mean aerodynamic chord, if wing alone)
$C_{M_q} + C_{M_{\dot\alpha}}$ = pitch damping moment coefficient, $[C_M(q)/(qd/2V_\infty) + C_M(\dot\alpha)/(\dot\alpha d/2V_\infty)]$
C_{M_α} = pitching moment coefficient derivative
C_N = normal-force coefficient
C_{N_B} = normal-force coefficient of body alone
$C_{N_{B(V)}}$ = negative afterbody normal-force coefficient due to canard or wing-shed vortices
$C_{N_{B(W)}}$, $C_{N_{B(T)}}$ = normal-force coefficient on body in presence of wing or tail
$C_{N_{T(V)}}$ = negative normal-force coefficient component on tail due to wing or canard-shed vortex
$C_{N_{W(B)}}$, $C_{N_{F(B)}}$ = normal-force coefficient of wing or fin in presence of body
C_{N_α} = normal-force coefficient derivative
$(C_{N_\alpha})_W$, $(C_{N_\alpha})_T$ = normal-force coefficient slope of wing or tail, respectively
C_{P_B} = base pressure coefficient
C_T = thrust coefficient
d_j, d_{ref} = diameter of nozzle exit and reference body diameter, respectively, ft
F_6, F_8 = empirical factors used to represent aerodynamics of six and eight fins based on four-fin aerodynamics
h = altitude, ft
I = nondimensional base bleed injection parameter
$K_{B(W)}$, $K_{B(T)}$ = ratio of additional body normal-force coefficient in presence of wing, or tail to wing, or tail alone normal-force coefficient where δ is 0 deg
$K_{W(B)}$, $K_{T(B)}$ = ratio of normal-force coefficient of wing or tail in presence of body to that of wing or tail alone where δ is 0 deg
k = parameter used to define corner radius for squares and triangles, r_n/W_M
$k_{B(W)}$, $k_{B(T)}$ = ratio of additional body normal-force coefficient due to presence of wing or tail at a control deflection to that of wing or tail alone where α is 0 deg
$k_{W(B)}$, $k_{T(B)}$ = ratio of wing or tail normal-force coefficient in presence of body due to a control deflection to that of wing or tail alone where α is 0 deg
M_∞, M_j = freestream and jet exit Mach numbers, respectively
p_c, p_∞ = pressure in rocket motor chamber and freestream, respectively, lb/ft^2
QE = elevation angle at launch, deg
RMF = jet momentum flux ratio
r = local body radius, ft
r_{eq}, d_{eq} = radius and diameter, respectively, of a circular cross section body that has same cross-sectional area as that of noncircular cross section body, ft

Received 15 April 2002; revision received 6 March 2003; accepted for publication 3 July 2003.

*President, 9449 Grover Drive, Suite 201; drfgmoore@hotmail.com. Associate Fellow AIAA.
†Aerospace Engineer, Weapons Systems Department, Missile Systems Division, Dahlgren Division. Member AIAA.

r_n = corner radius of a rounded corner on a square or triangle, ft
s = wing or tail semispan plus the body radius in wing–body lift methodology, ft
T = thrust, lb
T_j = temperature at nozzle exit,° R
t_{BO} = time when engine burns out, s
W_m = maximum diameter of a triangle or square as measured normal to the velocity vector, ft
W_0, W_{BO} = initial and burnout weight, respectively, lb
X_{CP} = center of pressure in x direction, ft, or calibers from some specified reference point
x_j = location of nozzle exit with $x_j = 0$ being at base of rocket, ft
α = angle of attack, deg
γ_j = ratio of specific heats at nozzle exit
$(\Delta C_A)_f$, $(\Delta C_N)_f$, $(\Delta C_M)_f$ = change in axial, normal, and pitching moment coefficients, respectively, due to a flap deflection δ_f
δ_f = control deflection of trailing edge flap, positive trailing edge down, deg
δ_W, δ_T = deflection of wing or tail surfaces, positive leading edge up, deg
θ_f = flare angle, deg
Φ = roll position of missile fins, where 0 deg corresponds to fins in the plus orientation and 45 deg corresponds to fins rolled to the cross orientation, deg

Introduction

THE aeroprediction code (APC) has been developed over a 30-year period beginning in 1971. The objective of the APC development over this 30-year period has stayed the same: to predict aerodynamics cost effectively and with reasonable accuracy over the flight envelope and configuration geometries of interest to weapons designers. Although the objective of the APC has stayed the same, the application uses, flight requirements, and configuration geometries have evolved over that time frame. The initial application was primarily to obtain accurate range estimates of various unguided projectile design concepts at low angles of attack (AOA) and Mach numbers less than 2.5. Now the application includes trim aerodynamics of guided weapons, aerodynamic design of guided weapons, structural loads, and aerodynamic heating. Mach numbers as high as 15 have been encountered, AOA as high as 90 deg, and body geometries axisymmetric or nonaxisymmetric have been considered in the design process. Figure 1 summarizes the current objective, application, and flight requirements of the APC effort.

The primary focus of this paper is to summarize the new technology that has been integrated into the APC 1998 (AP98) to form the basis of the APC 2002 (AP02). As already mentioned, the APC has evolved over a 30-year period with eight different versions developed (AP72, AP74, AP77, AP81, AP93, AP95, AP98, and AP02). Many references may be found in the literature summarizing the technology developed as part of the first seven versions of the APC. For the convenience of the many users and others in the aerodynamic community, these references are summarized in Ref. 1. The first three versions of the APC focused on meeting guided and unguided projectile requirements, whereas the next four versions focused on meeting missile requirements. During the past 20 plus years, many emerging projectile concepts have been investigated; however, many could not be considered in their entirety by the APC. The APC could be used as the workhorse to do many of the aerodynamic calculations, but the projectile concepts had many design needs that could not be met with the previous version of the APC, the AP98. These emerging projectile needs that form the basis of the AP02 are summarized in Fig. 2, with the date each new technology was developed given in parentheses.

OBJECTIVE

PREDICT AERODYNAMICS COST EFFECTIVELY AND WITH REASONABLE ACCURACY OVER FLIGHT ENVELOPE OF INTEREST TO WEAPONS DESIGNERS

APPLICATION REQUIREMENT OF APC

- INPUTS TO 3-DOF/TRIM PERFORMANCE MODELS
- AERODYNAMIC DESIGN (PRELIMINARY)
- PRELIMINARY STRUCTURAL LOADINGS
- CONVECTIVE HEAT TRANSFER INPUTS

OVERALL FLIGHT REQUIREMENTS

MACH NUMBER:	0-15
ANGLE-OF-ATTACK:	0-90 deg
CONTROL DEFLECTION:	±30 deg
ROLL ORIENTATION:	0 deg, 45 deg
SETS OF FINS:	0, 1, 2 REQUIRED; 3 DESIRED
BODY GEOMETRY:	AXISYMMETRIC REQUIRED; NONAXISYMMETRIC TREATMENT DESIRED

Fig. 1 Objective and requirements of APC.

With reference to Fig. 2, the first requirement that we addressed for the projectile concepts was that of providing aerodynamics for concepts that consider six and eight fins as alternatives to two or four fins, which the AP98 handled. The extended range guided munitions (ERGM), as well as other concepts, have considered multifins in the past. New technology was developed[2,3] and integrated into the AP98 to automate the multifin aerodynamics computation process.

The next problem area addressed for the projectiles was refinement of the nonlinear aerodynamic terms. The primary database on which these nonlinear terms were developed was the NASA Tri Service Data Base.[4] The Ref. 4 database was developed using a constant value of r/s of 0.5, which is typical of many missiles. However, many guided projectiles have fins with fairly large semispans and can have r/s values as low as 0.2. A more recent database[5] was provided to us where r/s was varied from 0.25, 0.33, and 0.5. This new database allowed us to refine our nonlinear aerodynamic terms for all normal force and interference effects. The new technology resulting from the refinement was documented[6–8] and integrated into the AP98.

The third problem area indicated in Fig. 2 for projectiles was dynamic derivatives. The dynamic derivatives had not been changed since 1977. The problem areas include no pitch damping term for the flare component of a projectile, the body-alone pitch damping was based on an old empirical database, and no nonlinear terms were included in the dynamic derivative computation process. The first two of these problem areas were addressed, improved on, documented,[9,10] and integrated into the AP98 to be a part of AP02. The third problem area, no nonlinearities included for the dynamic derivatives, was not addressed due to lack of a good generic database that covered the flight regimes of interest. To develop a generic database, analogous to Ref. 4 or 5, was beyond the scope of the present work.

The fourth problem area addressed for the projectile needs was that of improving the power-on base drag and providing a base bleed capability. The power-on base drag was incorporated in the AP81 and had not been changed since that time. This methodology was improved on by making it more robust. In addition, a base bleed capability, which has been requested by projectile designers for over 10 years, was integrated into the APC and will also be a part of the AP02. The improved power-on base drag methodology was documented in Refs. 11 and 12.

Another area indicated for improvement in Fig. 2 to meet projectile requirements is that of improving the zero lift axial force for noncircular cross section bodies. Some weapon concepts, such as the mission responsive ordnance, need the capability to predict axial force reasonably and accurately so that a good trajectory estimate can be made. Some modifications to axial force for nonaxisymmetric bodies were made and incorporated into the AP98.[13] However, without adequate data, it was not clear if enough refinements in axial

Table 1 Evolution of aeroprediction code in terms of major new added capability

Version	Weapons	Aerodynamics	Flight conditions: Mach no.	Real gas available	AOA range, deg	Roll, deg	Trajectory available	Nonlinear distributed loads available	Computers	Emerging projectile needs
1972	Axisymmetric unguided projectiles	Static only	0–3	No	0–15	$\Phi = 0$	No	No	CDC	No
1974	Axisymmetric unguided projectiles, rockets, missiles	Static only	0–3	No	0–15	$\Phi = 0$	No	No	CDC	No
1977	Axisymmetric unguided projectiles, rockets, missiles	Static and dynamic	0–3	No	0–15	$\Phi = 0$	No	No	CDC, IBM	No
1981	Axisymmetric unguided projectiles, rockets, missiles	Static and dynamic	0–8	No	0–15 (Limited conf at higher α)	$\Phi = 0$	No	No	CDC, IBM, VAX	No
1993	Axisymmetric unguided projectiles, rockets, missiles	Static and dynamic	0–20	Yes	0–30	$\Phi = 0$	No	No	CDC, IBM, VAX Silicon Graphics	No
1995	Axisymmetric unguided projectiles, rockets, missiles	Static and dynamic	0–20	Yes	0–90	$\Phi = 0$	No	No	Interactive personal computer	No
1998	Axisymmetric and asymmetric missiles, rockets	Static and dynamic	0–20	Yes	0–90	$\Phi = 0, 45$	No	Yes	Interactive personal computer, Windows 98 only	No
2002	Same plus multifin	Static and dynamic	0–20	Yes	0–90	$\Phi = 0, 45$	Yes	Yes	Improved interactive personal computer, Windows 98, 2000, and NT	Yes

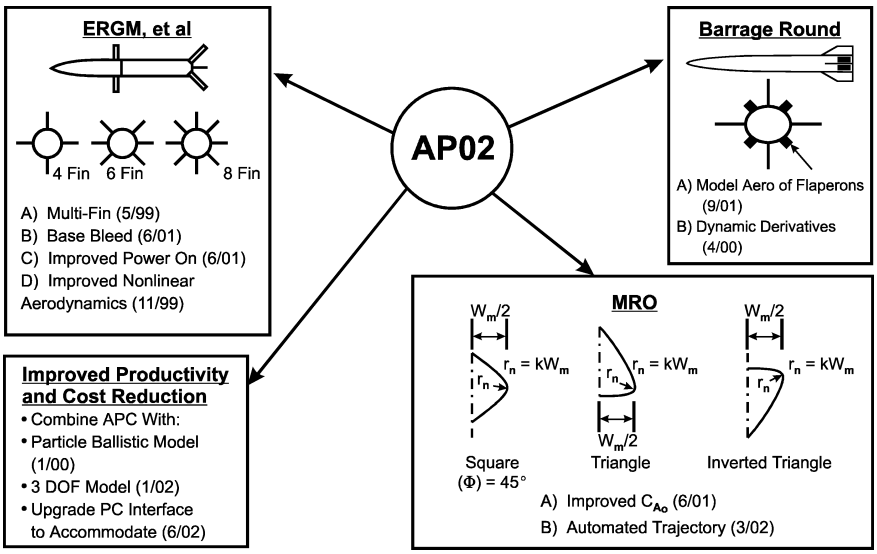

Fig. 2 AP02 requirements.

force had been made. A recent database taken at the Aeroballistic Range Facility[14] at Eglin Air Force Base has allowed the axial force prediction for noncircular bodies to be refined.

The final aerodynamic requirement referred to in Fig. 2 that the AP98 cannot meet is to calculate aerodynamics of concepts that use trailing-edge flaps for control. The barrage round is an example of a concept that considered trailing-edge flaps. Again technology was developed and documented[15] and will be a part of the AP02. This new technology can only be applied to the aft-located set of lifting surfaces as presently configured for the AP02.

In addition to aerodynamic needs that were not met from a projectile requirements standpoint, improved productivity for one of the primary applications of the APC aerodynamics is addressed by the AP02. This application is to use aerodynamics generated by the AP02 as inputs to trajectory (either ballistic or trim mode) analysis. The AP98 process is to generate a set of aerodynamics and provide these to a flight dynamicist, who will input the aerodynamics into a trajectory module and generate trajectories. In many cases, aerodynamic design changes are made as a result of this process, and an interaction process between the aerodynamicist and flight dynamicist begins. The AP02 will contain a module for ballistic and a three-degree-of-freedom (3-DOF) code for trim aerodynamics. As a result, a personal computer can be used to make design changes rapidly, and the results in terms of range be seen. This automation of incorporation of trajectories into the AP02 should provide significant productivity improvements.

Table 1 summarizes the APC evolution from its inception in 1972 to the present AP02 version that is now available. For more details of the AP02 theory in Table 1, see Refs. 1 and 16.

AP02 New Capability

In the Introduction, the new capability that was added to the AP98 that makes up the AP02 from a needs and requirements standpoint was discussed. In this section, the technical approach used to develop each new method discussed in the Introduction is discussed without

going into details. For details of each of the new methods, see Refs. 2, 3, 6–13, 15, and 16.

Multifin Aerodynamics[2,3]

Multifin here refers to six- or eight-fin configurations because the AP98 currently has two- or four-fin aerodynamic prediction capability. To keep the cost to integrate the multifin capability into the AP98 down, we were led to the definition of factors by which the two- or four-fin aerodynamics could be multiplied to represent the aerodynamics of six or eight fins.

The multifin aerodynamics we are interested in include the effect on axial force, normal force, center of pressure, roll damping moment, and pitch damping moment. Magnus moment is presently assumed to be zero for fin-stabilized weapons because of low spin rates. (This assumption may be inaccurate if the spin rate is greater than a few cycles per second.) Each of these aerodynamics will be considered individually.

Based on past experience with calculations of axial force of two fins vs four fins, we have found reasonable accuracy by taking the axial force coefficient of a single fin and multiplying it by the number of fins of interest. No interference effect between the body and fins, other than the base pressure, has been observed. Hence, this assumption was made for the axial force of weapons with more than four fins, that is,

$$C_A = C_{A_{\text{body}}} + \left(C_{A_{\text{SF}}}\right)(\text{NF}) \tag{1}$$

where NF is the number of fins. However, note that, as the number of fins increases from four to eight, the probability of mutual interference between fins increases. This is particularly true for highly blunt fin leading edges. Nevertheless, for the time being, Eq. (1) was assumed.

It was also assumed that the center of pressure of the total normal force contribution of multifins is the same as that of four fins. The total normal-force contribution of the fins includes the normal force of the fins in presence of the body, plus the additional normal force on the body as a result of the fins being present.

Slender body theory (SBT) states that the normal force of six and eight fins is, respectively, 1.5 and 2.0 times that of four fins. Experience has shown these factors to be high in general, particularly as AOA increases. Because AP98 has all of the nonlinearities for the normal force contributions of the wing, body, and interference terms, it was assumed that

$$\left[C_{N_{W(B)}}, C_{N_{B(W)}}, C_{N_{T(V)}}\right]_{6,8\text{ fin}} = (F_6, F_8)\left[C_{N_{W(B)}}, C_{N_{B(W)}}, C_{N_{T(V)}}\right]_{4\text{ fin}} \tag{2}$$

where the factors F_6 and F_8 were determined. F_6 and F_8 are the factors by which we multiply the cruciform fin normal-force components for six- and eight-fin configurations, respectively. These factors are the SBT factors of 1.5 and 2.0 already mentioned. However, the SBT values were replaced with values appropriate for a given aspect ratio wing at a given AOA and Mach number. Whereas the factors were determined explicitly for the wing–body plus the body–wing contributions to normal force, they were also assumed to apply to the tail downwash $C_{N_{T(V)}}$ and pitch damping moment. Computational fluid dynamics (CFD) methods were used to calculate the factors F_6 and F_8 of Eq. (2).

For roll and pitch damping moments, the damping moments of the planar fins are computed using linear theory. The number of fins (four, six, or eight) and the mutual interference effects of the fins onto the body are accounted for by SBT[17] for roll damping moment and by the same factors (F_6 and F_8) for the normal force [Eq. (2)] for pitch damping moment.

Aerodynamic Smoother[2,16]

The APC uses many different methods to predict aerodynamics at a given Mach number and AOA. At Mach numbers 1.2, 2.0, and 6.0, where one method ends and another method takes over, discontinuities in aerodynamics can be obtained. The discontinuities are the result of different methods being used on either side of $M_\infty = 1.2$, 2.0, or 6.0. The problem does not appear to be significant at $M = 1.2$, but at 2.0 and 6.0, these fictitious discontinuities can be misleading to an unsuspecting user of the APC when they plot the aerodynamics as a function of Mach number.

The user is left with the question of which number is best to use at the transition points. For example at Mach 2, is it better to use the value of aerodynamics at Mach 1.99 or Mach 2.01? Experience has shown, in comparison to data, that an average of the two numbers is probably better than using either of the estimates alone. As a result, an aerodynamic smoother was developed that is based on an average of the values given by second-order shock expansion (SOSE) and second-order Van Dyke (SOVD) at $M = 2.0$ and an average of SOSE and modified SOSE (MSOSE) at $M = 6.0$. The smoother linearly goes to the SOVD value at $M = 1.5$ and to the SOSE value of the particular coefficient at $M = 2.5$. Likewise, the value of the aerodynamic coefficient at $M = 5.0$ is based fully on SOSE. At $M = 7.0$, it is based on MSOSE. The average value of the two methods is used at $M = 6.0$.

Improved Nonlinear Aerodynamics[6–8]

The APC is a semiempirical code that predicts low AOA aerodynamics primarily based on linearized, slender body, and local slope theories and computes the nonlinear terms empirically based on several large component wind-tunnel databases.[4,5,18,19] To illustrate the semi-empirical approach, it is convenient to write the total normal force coefficient equation for a wing–body–tail configuration as defined by Pitts et al.[20] That is,

$$\begin{aligned} C_N = {} & C_{N_B} + \left[\left(K_{W(B)} + K_{B(W)}\right)\alpha + \left(k_{W(B)} + k_{B(W)}\right)\delta_W\right]\left(C_{N_\alpha}\right)_W \\ & + \left[\left(K_{T(B)} + K_{B(T)}\right)\alpha + \left(k_{T(B)} + k_{B(T)}\right)\delta_T\right]\left(C_{N_\alpha}\right)_T \\ & + C_{N_{T(V)}} + C_{N_{B(V)}} \end{aligned} \tag{3}$$

Each of the terms in Eq. (3) is composed of a linear and a nonlinear term. In Ref. 20, only the linear term is considered, whereas more recent semi-empirical codes include nonlinearities as well.[21]

The nonlinear terms of the AP98 were based primarily on databases,[4,18,19] where r/s was a constant value of 0.5. A more recent missile component database[5] varies r/s from 0.25, 0.33, and 0.5. This more recent database, which includes wing-alone, body-alone, and wing–body data, allows refinement in the nonlinear terms that are used in the AP98 to model Eq. (3) and the companion center of pressure representation.

When the AP98 was compared to the Ref. 5 database, it was found that there was good agreement between theory and data. The average error on normal force and center of pressure was about 7 and 2% of the body length, respectively.[6] Although these comparisons are within the desired accuracy levels of ±10 and ±4% of body length for normal force and center of pressure, respectively, there were some areas where the AP98 accuracy compared to the Ref. 5 database seemed to warrant improvement. These areas were body-alone normal-force coefficient for $M_\infty > 2.75$, body-alone center of pressure in the transonic Mach number region, and the treatment of the linear term of the body-alone normal-force coefficient above $\alpha = 30$ deg. For the wing-alone and total configuration aerodynamics, some slight changes appeared to be needed in the wing-alone aerodynamics and wing–body interference factors due to both angle of attack and control deflection.

Once the aforementioned refinements in the nonlinear aerodynamics methodology were incorporated into the AP98 to form the basis of the AP02, the code was then compared to several cases within the databases[4,5] on which the refinements were based. It was found the refinements based on the new database[5] allowed the average normal-force error to be reduced from 7 to 4% or about a 40% reduction in error. There was also some slight improvement in center of pressure noted, but the improvements were not quantified as with the normal-force coefficient. For the details of the nonlinear aerodynamics improvements, see Refs. 6–8 or Ref. 16 for a summary of the changes.

Improved Pitch Damping with Emphasis on Configurations with Flares[9,10]

The next area that new technology has been added to the AP98, which will be a part of the AP02, is improvement in aerodynamics of flared configurations, particularly the pitch damping derivative. The problem of inaccurate aerodynamic predictions for flared configurations from the APC first came to our attention several years ago in the form of pitch damping moment coefficient predictions for a flared projectile concept. The increased interest in the use of flares for stability in recent years, particularly for higher Mach numbers for example, Refs. 22–24, has also led the present authors to feel that improvements in the aerodynamic predictions of flared projectiles were needed.

As a result of the increased interest in flared projectiles for higher Mach number applications, the present authors examined the APC to determine its weak areas with respect to flared shaped projectiles. Several problem areas were identified. First, for the static aerodynamics, no particular attention was given for flared projectiles for $M_\infty < 1.2$. For $M_\infty \geq 1.2$, low AOA aerodynamics were computed by theoretical methods such as SOVD or SOSE theory (SOSET) and reasonable estimates of static aerodynamics (C_A, C_N, and x_{CP}) could be obtained from the APC. For $M_\infty < 1.2$, the capability to compute static aerodynamics needed to be incorporated into the code.

The second problem uncovered in the APC was for the dynamic derivative, $C_{M_q} + C_{M_{\dot\alpha}}$, or pitch damping moment coefficient. No capability existed at any Mach number in the APC for pitch damping moment of flared projectile shapes. In fact, based on recent CFD calculations of projectiles without a flare,[25,26] it was found that the pitch damping moment of configurations without flares needed improvement as well.

All three of the weak areas of the AP98 with respect to aerodynamics of flared shaped projectiles were improved on and are a part of the AP02. The method of Wu and Aoyoma[27] was used for transonic static aerodynamics of a flare, SBT for subsonic Mach numbers and exact theory[28] for supersonic Mach numbers. Pitch damping improvements were then made on the body alone empirically based on the CFD results from Refs. 22, 23, 25, and 26. Finally, pitch damping of the flare was estimated by using an approach similar to that used in Ref. 29 for the wing and by replacing the wing with a flare. In Refs. 9 and 10 the details of the methodology for aerodynamics of a body with a flare are given.

Improved Power-on Base Drag Prediction Including Base Bleed Effects[11,12]

The approach used in the AP98 to predict the effect of the rocket engine burning on the base drag of weapons was integrated into the APC in the late 1970s and had not been upgraded since that time. The method utilized was basically an extension of the Brazzel and Henderson[30] technique (also see Ref. 1). The technique of Brazzel and Henderson[30] was for solid rockets, which had an exit Mach number of 1.0 or greater. It required knowledge of some of the details of the rocket such as chamber pressure, exit area to nozzle throat area, specific heat ratio of the exit gas, and location of the nozzle exit with respect to the base of the missile or projectile. This approach has been shown to give reasonable estimates of power-on base drag for a limited range of flight conditions when the parameters P_c/P_∞, A_j/A_t, γ_j, and x_j/d_r are known.

Although the approach by Brazzel and Henderson[30] has its strengths, it also has several weaknesses when approached from an aerodynamics viewpoint. First, it was limited to jet momentum flux ratios (RMF) of about 2.5 or less. Many of the world's rockets have values of this parameter much higher, and therefore, the method of Brazzel and Henderson was extended to higher values of RMF. This extension to higher values of RMF was documented in Ref. 1. Another problem with the Brazzel and Henderson technique from an aerodynamicist's viewpoint is the required knowledge of the engine parameters. These parameters are required to perform conceptual design tradeoffs of various rockets for total drag when the engine is burning. As a result of this desire for conceptual trade studies where some account of engine-on base drag is considered, other simplified procedures are needed for base drag prediction. Two other options were therefore defined to calculate power-on base drag. Another limitation of the Brazzel and Henderson method is its limitation to supersonic flow at the nozzle exit. Although the exit supersonic flow requirement is not a severe limitation for most rocket engines, it is a severe limitation for projectile configurations that use base bleed for base drag reduction. As a result of this shortcoming, a method developed by Danberg[31] for predicting base drag for small values of the bleed injection parameter I was made more general. A final limitation of the Brazzel and Henderson[30] method is that it was derived based on freestream Mach number data of 1.5 and greater. Therefore, the modified Brazzel and Henderson method was extended to the transonic Mach number regime.

The modifications to the Brazzel and Henderson[30] (see also Ref. 1) and Danberg[31] methods were incorporated into the APC for power-on base drag prediction and are a part of the AP02. The power-on base drag modifications will also be incorporated into the personal computer interface for the AP02 to allow the various power-on options to be considered in a very user friendly mode. The detailed theory associated with the modifications to the Brazzel and Henderson[30] and Danberg[31] methods may be found in Refs. 11 and 12.

Improved Zero-Lift for Axial Force for Noncircular Bodies[16]

The approach used in the AP98 for calculating drag of the nonaxisymmetric body configurations is based on the formation of an equivalent axisymmetric body of the same cross-sectional area. A correction is made in the skin-friction component, where

$$\left(C_{A_f}\right)_{\mathrm{NC}} = \left[\frac{(\mathrm{cir})_{\mathrm{NC}}}{2\pi r_{\mathrm{eq}}}\right]\left(C_{A_f}\right)_{\mathrm{eq}} \tag{4}$$

The subscripts NC and eq represent the noncircular and equivalent circular body, respectively. However, wave drag and base drag were based on the equivalent body, which assumes an equal area distribution.

To check out the validity of these assumptions on the drag of nonaxisymmetric bodies, a series of ballistic range tests were conducted at the Aeroballistic Range Facility (ARF), Eglin Air Force Base. These test results are documented in Ref. 14. The models tested included three- and four- fin circular and elliptical configurations with $a/b = 1.25$ and 1.67 and four-fin square and three-fin triangular cases. Also, 11–18 shots of each configuration was tested, all with a constant cross-sectional area and with an equivalent diameter of 17 mm.

When the AP98 axial force prediction was compared to those of the ARF test results, it was found the predictions for the elliptical cross section configurations gave acceptable accuracy, whereas the predictions for square and triangular configurations needed some slight improvements. An empirical formula was derived for the square cross section shape, which modified the wave and base drag term [in addition to Eq. (4)] of the equivalent axisymmetric body a small amount. This equation is given by

$$(C_A)_{\mathrm{sq}} = \left(C_{A_f}\right)_{\mathrm{eq}}\left[\frac{(\mathrm{cir})_{\mathrm{sq}}}{2\pi r_{\mathrm{eq}}}\right] + \left(C_{A_W} + C_{A_B}\right)_{\mathrm{eq}}[1 + 0.08(1 - 2k)] \tag{5}$$

In Eq. (5), the sq and eq subscripts represent the square and equivalent circular body, respectively. Also, the axial force of the triangular cross section shape modified the base drag term in addition to Eq. (4). This equation is given by

$$(C_A)_{\mathrm{tr}} = \left(C_{A_f}\right)_{\mathrm{eq}}\left[\frac{(\mathrm{cir})_{\mathrm{tr}}}{2\pi r_{\mathrm{eq}}}\right] + \left(C_{A_B}\right)_{\mathrm{eq}}[1 + .07(1 - 2k)] + \left(C_{A_W}\right)_{\mathrm{eq}} \tag{6}$$

In Eq. (6), the subscript tr represents the triangular cross section.

Equations (5) and (6) resulted in axial force coefficients that were in closer agreement to data than the AP98 predictions. The details

of the improved axial force prediction for nonaxisymmetric bodies including several comparisons to experimental data are given in Ref. 16. Equations (5) and (6) are a part of the AP02 methodology.

Trailing-Edge Flap Technology[15]

One idea that has been considered to meet lower cost, lower volume, and lower maneuverability control requirements for guided projectiles is to deflect a part of a wing or tail surface as opposed to the entire surface. The portion of the tail surface considered for deflection is at the tail or wing trailing edge. The most recent version of the APC (AP98)[21] distributed to users is not capable of computing aerodynamics on a concept when the trailing-edge flap is deflected for control. As a result of this deficiency and a requirement in the guided projectile community, new technology was developed for the AP02 that allows trailing-edge flaps to be deflected for control.

The approach taken for the AP02 technology was to define a total wing deflection that gave a normal force equal to that of a flap deflected an amount δ_f, that is,

$$\delta_W = f(\delta_f) \tag{7}$$

The Eq. (7) approach is similar to that used in the Missile DATCOM.[32]

Although the approach used by in Missile DATCOM [Eq. (7)] to compute aerodynamics of trailing-edge flaps is the same approach that was adopted for use here, the methods that were used for the AP02 differ from those[33,34] used in the Missile DATCOM.[32] There are several reasons for this difference in methods. First, the method of Goin[34] had too many limitations. Some of these limitations include that there were requirements for supersonic leading and trailing edges of the flap hinge line, viscous effects were not accounted for, and the method of Goin did not include nonlinearities due to large flap deflections or AOAs. Second, although the method in Ref. 33 takes into account some of the viscous and nonlinear effects that the method in Ref. 34 does not account for, the method itself is inconsistent with that of Ref. 34.

The method derived for the AP02 used linearized theory at low AOA, the nonlinear aerodynamic approximations discussed earlier at high AOA, and experimental databases[35,36] to determine empirical relationships needed to help define δ_W as a function of δ_f according to Eq. (7). A shift in the center of pressure of the total wing was derived empirically to account for viscous effects and the fact the flap is deflected vs the full wing. Also, an approximate correction was made to the axial force to account for the difference arising from the wing vs the flap being deflected. For details of the trailing-edge flap method, see Ref. 15.

Trajectory Models[16]

The evaluation of the flight performance of today's projectiles and missiles is typically a two-step, iterative process. First, the aerodynamic coefficients for the airframe must be determined over the anticipated envelope of flight conditions through wind-tunnel testing or by using software that will predict the aerodynamics. Second, the aerodynamic coefficients are inserted into a trajectory model so that the aerodynamic forces acting on the missile may be determined for any flight condition. The trajectory model is then executed, and the results are analyzed.

In the preceding process, the first step is usually performed by an aerodynamicist, whereas the second step is performed by a flight dynamicist. If the flight dynamicist is not satisfied by the flight performance predicted by the trajectory model, changes may be made to the airframe. These changes will in turn effect the aerodynamics, thereby requiring the aerodynamicist to create a new set of aerodynamic data to be inserted into the trajectory model. This iterative process continues until an airframe is found that optimizes some desired aspect of the flight performance.

Depending on the flight regime over which the aerodynamics are to be computed, a set of trim aerodynamics may take on the order of 1 to 2 workdays to generate. The term trim means that the aerodynamic coefficients correspond to a state in which the pitching moment coefficient C_M is equal to zero. As an example, a set of trim aerodynamics was found for a wing–body–tail configuration for AOA α ranging from 0 to 30 deg in 5-deg increments. Also, there were two center of gravity locations and four Mach numbers M to be evaluated. The product of the AOA, c.g. location, and Mach numbers means that there were 56 trim points to be found. The work was performed using AP98. Although AP98 executes fairly rapidly, it does not directly provide trim aerodynamics. Instead, the user must generate plots of pitching moment vs fin deflection δ at a given Mach number and AOA. Then the user must eyeball the results until the trim point is found to be within some desired accuracy. This may entail several iterations until the $C_M = 0$ point is bounded and is displayed on a scale large enough to ensure accuracy. It took an experienced AP98 user approximately 10 h to accomplish the task. Of the 10 h, only about 15 min were required to set up the missile configuration in AP98.

Note that the run matrix of 56 points is a very modest one. For example, the effect of altitude on trim axial force coefficient $(C_A)_{\text{trim}}$ was disregarded. Also, the intervals between Mach numbers and AOA were fairly coarse. The c.g. corresponded to the full and empty fuel states only. To predict flight performance more accurately, a correspondingly more detailed set of aerodynamics must be provided. The generation of aerodynamic tables, especially trim aerodynamics, can be tedious and time consuming.

The insertion of aerodynamics into the trajectory model also requires some amount of time. The actual amount of time will depend on the amount of aerodynamic data to be inserted, as well as the experience level of the flight dynamicist. For example, it took about 2 h to insert the aforementioned set of trim aerodynamics into a trim 3-DOF model. This time also included the compilation and execution of the code. In this case, the flight dynamicist was experienced with the particular trajectory model. Obviously, the insertion of aerodynamic data would take considerably longer had the users not been familiar with the trajectory model.

The total amount of time to generate a set of aerodynamics, insert the aerodynamics into a trajectory model, and run the trajectory model for this example was approximately 12 h and required two people. Each person was experienced in performing part of the task. Also, each person was available to do the work when required. That is, there was no delay when the aerodynamicist transitioned the aerodynamic data to the flight dynamicist. In summary, one iteration from aerodynamicist to flight dynamicist for the example case cited took approximately 12 h. This is relatively quick turn around time because the aerodynamics were sparse (in terms of Mach numbers and control deflections selected) and the people doing the work were experienced and available.

The process discussed in the preceding paragraph was for one iteration only. If the performance of the concept was adequate, that would probably complete the initial phase of the design and aerodynamic and performance assessment of the concept in question. However, in most cases, several design iterations are required to see the effect on the aerodynamics and performance of each design change. Thus, the time involved to generate the trim aerodynamics and perform performance assessments is a minimum of 12 h times the number of concepts investigated. Combining the APC with trajectory models for automatic trajectory generation of a given design concept, thus, has potential for a large cost savings. When the cost savings is multiplied by the many users of the APC, the cost savings becomes even larger.

As a result of the desire to reduce time and cost for design and performance trade studies, a 2-DOF ballistic model[37] and a trim 3-DOF model[38] were combined with the APC and are part of the AP02. When AP02 code is used, the aforementioned example case can be performed in 1 h vs 12 h, with one person vs two people. More details of the implementation of the trajectory models with the AP02 may be found in Ref. 39.

Upgraded Pre- and Postprocessor

The AP95, AP98, and AP02 have all utilized a pre- and a postprocessor for inputs and outputs. The pre- and postprocessors significantly reduced the amount of time to get a set of aerodynamics for

a given configuration. With the addition of trajectory model options and many new technologies incorporated into the AP02, the preprocessor was modified substantially to allow all of the options to be effectively utilized. Also, many additional plots are available, particularly for the trajectory models, in the postprocessor. Also, the AP02 pre- and post-processor will be compatible with Microsoft Windows 98, 2000, and NT software. The AP98 was compatible with Windows 98 only.

Summary of Theoretical Methods

The preceding section summarized the new methods that will be included in the AP02 that were not available in the AP98. See Refs. 1 and 21 for a summary of the methods that were part of the AP98. Suffice it to say that the AP98 is based on modified versions of SBT, linear theory, or second-order perturbation theories at low AOA and empirical methods at high AOA. The low AOA theoretical methods gives the APC a good foundation to predict aerodynamics

Table 2 AP02 methods for body-alone aerodynamics

	Mach number region				
Component	Subsonic $M_\infty < 0.8$	Transonic $0.8 \le M_\infty \le 1.2$	Low supersonic $1.2 \le M_\infty \le 1.8$	Moderate/high supersonic $1.8 \le M_\infty \le 6.0$	Hypersonic $M_\infty > 6.0$
Nose wave drag	Empirical	Semiempirical based on Euler solutions	SOVD plus modified Newtonion theory (MNT)	SOSET plus improved modified Newtonion theory (IMNT)	SOSET Plus IMNT modified for real gases
Boattail or flare wave drag	——	Wu and Aoyoma[27]	SOVD	SOSET	SOSET for real gases
Skin-friction drag			Van Driest II		
Base drag[a]			Improved empirical method[a]		
Power-off[a]			Empirical[a]		
Power-on[a]			Modified Brazzel and Henderson[30] method[a]		
Base bleed[a]			Modified Danberg method[a]		
Axial force at α			Empirical method		
Aeroheating information		——		SOSET plus IMNT for real gases	
Inviscid lift and pitching moment	Empirical	Semiempirical based on Euler solutions	Tsien first-order crossflow	SOSET	SOSET for real gases
Viscous lift and pitching moment			Improved Allen and Perkins crossflow		
Nonaxisymmetric Body aero[a]					
Lifting Properties[a]			Modified Jorgensen[a]		
Axial force[a]			Modified axisymmetric body[a]		
Nonlinear structural loads available ($\Phi = 0, 45$ deg)		NO		YES	

[a]New theories.

Table 3 AP02 methods for wing-alone and interference aerodynamics

	Mach number region				
Component	Subsonic $M_\infty < 0.8$	Transonic $0.8 \le M_\infty \le 1.2$	Low supersonic $1.2 \le M_\infty \le 1.8$	Moderate/high supersonic $1.8 \le M_\infty \le 6.0$	Hypersonic $M_\infty > 6.0$
Wave drag		Empirical	Linear theory plus MNT	Shock expansion (SE) plus MNT along strips	SE plus MNT for real gases along strips
Skin-friction drag			Van driest II		
Trailing-edge separation drag			Empirical		
Body base pressure caused by tail fins			Empirical		
Inviscid lift and pitching moment					
Linear	Lifting surface theory	Empirical	3-Dimensional thin wing theory (3DTWT)	3DTWT	3DTWT
Nonlinear			Empirical		
Wing–body, body–wing interference due to α ($\Phi = 0, 45$ deg)					
Linear			SBT or linear theory modified for short afterbodies		
Nonlinear[a]			Improved empirical[a]		
Wing–body, body–wing interference due to δ ($\Phi = 0, 45$ deg)					
Linear			SBT		
Nonlinear[a]			Improved empirical[a]		
Wing–tail interference ($\Phi = 0, 45$ deg)			Line vortex theory with modifications for $K_{W(B)}$ term and nonlinearities[a]		
Aeroheating		None present		SE plus MNT	SE plus MNT real gases
Nonaxisymmetric body aerodynamics ($\Phi = 0, 45$ deg)			Improved Nelson method		
Nonlinear structural loads available ($\Phi = 0, 45$ deg)		No		Yes	
6, 8 fin aerodynamics[a]					
Linear[a]			Slender body theory[a]		
Nonlinear[a]			Semi-empirical (cfd + data)[a]		
Trailing-edge flaps on tails[a]			Semi-empirical (seek tail deflection for equal normal force[a])		

[a]New theories.

Table 4 AP02 methods for dynamic derivatives

Component	Mach number region				
	Subsonic $M_\infty < 0.8$	Transonic $0.8 \le M_\infty \le 1.2$	Low supersonic $1.2 \le M_\infty \le 1.8$	Moderate/high supersonic $1.8 \le M_\infty \le 6.0$	Hypersonic $M_\infty > 6.0$
Body alone					
No flare[a]	Empirical[a]				
With flare[a]	Semiempirical[a]				
Wing and interference roll damping moment	Lifting surface theory	Empirical		Linear thin wing theory	
Wing magnus moment			Assumed zero		
Wing and interference pitch damping moment	Lifting surface theory	Empirical		Linear thin wing theory	

[a]New theories.

Table 5 Trajectory capability within APC

Simulation mode	AP72-AP98	AP02
Particle ballistic[a]	None	Yes[a]
3 DOF[a]	None	Yes[a]

[a]New theories.

for various geometries and for various flight conditions up to AOA of about 10 deg. The empirical methods that were developed based on several large databases extend the low AOA methods to 90-deg AOA.

A summary of the theoretical methods that make up the AP02 are shown in Tables 2–5. Table 2 gives the body-alone methods, Table 3 provides the wing and interference methods, Table 4 shows the dynamic derivatives, and Table 5 provides the trajectory options that are part of the AP02. The new theories that are part of the AP02 that were not included in the AP98 are indicated.

Table 1 shows the evolution of the APC from its initial version, the AP72, to the latest version to be released, the AP02. As seen in Table 1, the AP02 is the only version of the APC that provides a trajectory option, provides multifin capability, and addresses several emerging projectile requirements.

Results and Discussion

The results and discussion section of the paper will focus primarily on showing example cases of the new elements of technology that have been added to the AP98 that make up the new AP02. Focusing on the newer elements of the AP02 technology still requires use of the elements of the AP98 that have not been modified. To point out the differences between the AP02 and AP98, both results will be shown compared to experiment when available. In some cases, such as six- and eight-fin aerodynamics, trailing-edge flaps, base bleed, or trajectories, this is not possible because the AP98 does not have these capabilities available. Many more example cases are given in Ref. 16.

The first new AP02 technology we will consider is the improved nonlinear aerodynamics. In Ref. 16, six example cases plus a comparison of the AP98 and AP02 to the databases[4,5] on which the nonlinearities were based are considered. Because of paper length considerations, we will show only a summary error comparison of the AP02 and AP98 to the databases on which the nonlinear terms were based[4,5] and a portion of one of the example cases given in Ref. 16.

A summary of the comparison of normal-force coefficient predictions by the AP02 and AP98 to the Refs. 4 and 5 databases is given in Table 6. The Tri-Service database[4] consisted of Mach numbers 0.6, 0.8, 1.2, 1.5, 2.0, 2.5, 3.0, 3.5, and 4.5 with AOA up to 25–40 deg (depending on Mach number) and for $\Phi = 0$ and 45 deg roll. The highest aspect ratio fins ($AR = 4$) of the Tri-Service data base were very small, and so the data associated with those fins was not included in Table 6. Also, the aspect ratio 2.0 fin data of Ref. 4 was only included for Mach numbers 1.5 and greater for the same reason of small fin planform. The Ref. 5 database consisted of Mach numbers 0.6, 0.9, 1.2, 1.6, 2.0, 2.3, 2.96, and 3.95 for AOA from 0 to 20 or 30 deg (depending on Mach number) but at the roll position of $\Phi = 0$ deg only.

Table 6 Average normal-force coefficient errors of AP02 compared to combined databases[4,5]

Mach no.	No. points	Average error, %
0.6	89	5.5
0.8–0.9	95	7.2
1.2	102	3.7
1.5–1.6	172	2.6
2.0	168	3.3
2.3–2.5	166	2.8
2.96–3.0	167	3.6
3.5–3.95	163	4.2
4.5	108	3.2
Total	1230	3.8

The Table 6 errors were measured at $\alpha = 10$, 15, 20, 25 and 30 deg, where data were available. The error in Table 6 is defined by

$$\text{error}\,(\%) = \left(\left|C_{N_{\text{exp}}} - C_{N_{\text{theory}}}\right| \Big/ C_{N_{\text{exp}}}\right) \times 100 \tag{8}$$

The errors in Table 6 are then broken down by Mach number and then summed and averaged for all Mach numbers. The average normal-force coefficient error of 3.8% in Table 6 is about 2–3% lower than for the AP98. In other words, incorporation of the Ref. 5 database, which focused on variations in r/s, has allowed the average normal-force errors to be reduced by about 40% when comparing the AP02 to the AP98 and the databases on which the nonlinear aerodynamic terms were based.

No average error on center of pressure was made because of time constraints. However, note that the average center of pressure error for the AP98 on the NASA Tri-Service database was less than 2% of the body length.[21] Improvements made in normal force should only improve these already excellent predictions. Likewise, no improvements in axial force were sought because we were satisfied with the power-off predictions of axial force from the AP98.

Whereas the average accuracy comparisons of C_N to experiment of Table 6 is impressive for a semiempirical code, the true measure of success is based on the ability to predict accurately aerodynamics on a wide variety of configurations outside the databases on which the empirical nonlinearities were derived. The one partial example from Ref. 16 shown here is a model of an older version of the SEASPARROW missile. A fairly extensive database exists for this configuration. The configuration is shown in Fig 3; the wings or tail surfaces can be used for control.

The Fig. 3 configuration has a length of about 18 calibers with a tangent ogive nose 2.25 calibers in length, and it has wings and tails of fairly high aspect ratio of 2.8 and 2.6, respectively. Data were taken at Mach numbers of 1.5–4.63 for AOAs to 40 deg and control deflections of 0 and 10 deg (at M of 1.5 and 2.0) and 0–20 deg (at M of 2.35–4.63). The data were taken at a Reynolds number of 2.5×10^6/ft, and boundary-layer trips were also used. The model had a hollow chamber, and chamber axial force measurements were

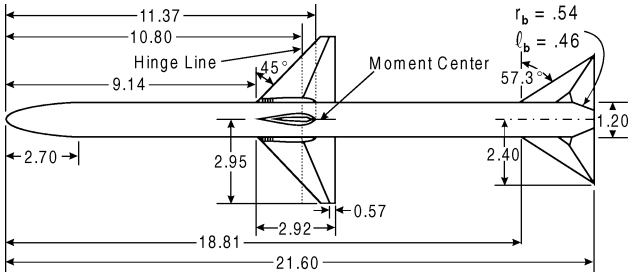

Fig. 3 Wing–body–tail configuration used in validation process (all dimensions in inches).

given separately in Ref. 40. These results were added to the forebody axial force measurements to compare with the AP98 and AP02.

Figure 4 shows the comparisons of the AP98 and AP02 to the data of Ref. 40 for $\Phi = 0$ and 45 deg at $M_\infty = 2.87$ (other cases in Ref. 16) and for the wing control configuration. Figures 4a and 4b give C_A, C_N, and C_M for $M_\infty = 2.87$ at $\delta_W = 0$ and $\delta_W = 20$ deg at $\Phi = 0$ deg. In general, both the AP98 and AP02 give good comparisons to data with the AP02 showing some slight improvement over the AP98.

Similar results to the $\Phi = 0$ deg case are shown in Figs. 4c and 4d for the $\Phi = 45$ deg roll orientation. Here again, both AP98 and AP02 show good agreement to experiment with the AP02 being slightly more accurate for all of the aerodynamic coefficients. Although not completely shown for brevity sake, in Ref. 16 the improvements of the AP02 over the AP98 shown in Table 6 is shown to be carried over to the example cases outside the databases on which the nonlinearities were based.

The next new technology incorporated into the AP02 is the multifin aerodynamics capability. Multifin here is meant six or eight fins because the AP98 already has the capability to handle two- and four-fin cases in the computational process. The case considered here is an U.S. Army six-fin projectile concept shown in Fig. 5a and taken from Refs. 22 and 41. The configuration in Fig. 5a consists of a cone–cylinder–body and is 13.99 calibers in length with a diameter of 1.39 in. The cone half-angle is 8 deg, and the leading and trailing edges of the fins are blunt. For the AP02 computations, Reynolds number was computed based on sea level conditions and the body diameter as reference length. The wind-tunnel model with no boundary-layer trip option was used in the AP02 for viscous flow computations. Ballistic data were available over a Mach number range from 3.0 to about 4.5. CFD data were given from $M_\infty = 3.0$ to 5.5, and AP02 computations were performed over this same Mach number interval.

Comparisons for normal-force coefficient and pitching moment coefficient slopes at zero AOA are shown in Fig. 5b. The AP02 results at lower Mach numbers tend to be somewhat high compared to the CFD numbers in both cases, and both tend to lie above the range data. Figure 5b also shows the comparison for axial force coefficient. Good agreement is obtained throughout in this instance. The comparison for pitch damping coefficient is also shown in Fig. 5b. Once again, the AP02 numbers are somewhat high relative to the CFD results, and both tend to lie above the majority of the ballistic data.

The next improvement in the AP02 is for configurations with flares. The case considered is taken from Ref. 22, and Fig. 6 gives pitch damping moment coefficient results for a configuration with a variable flare angle. As seen in Fig. 6, the AP02 gives good agreement to the Ref. 22 CFD results, whereas the AP98 gives acceptable predictions only for very small flare angles.

Two cases will be used to show the improvements in the AP02 with respect to predicting base pressure when the rocket engine is on or when a projectile burns a small amount of propellant in the base region. We will consider the base bleed case first. The case considered is shown in Fig. 7 (also see Ref. 42). The case is for a condition where $d_j/d_r = 0.31$, and $T_j = 2150^\circ$R at $M_\infty = 0.98$. Base pressure ratio is shown as a function of the injection parameter I. As seen in Fig. 7, excellent agreement of theory and experiment is seen.

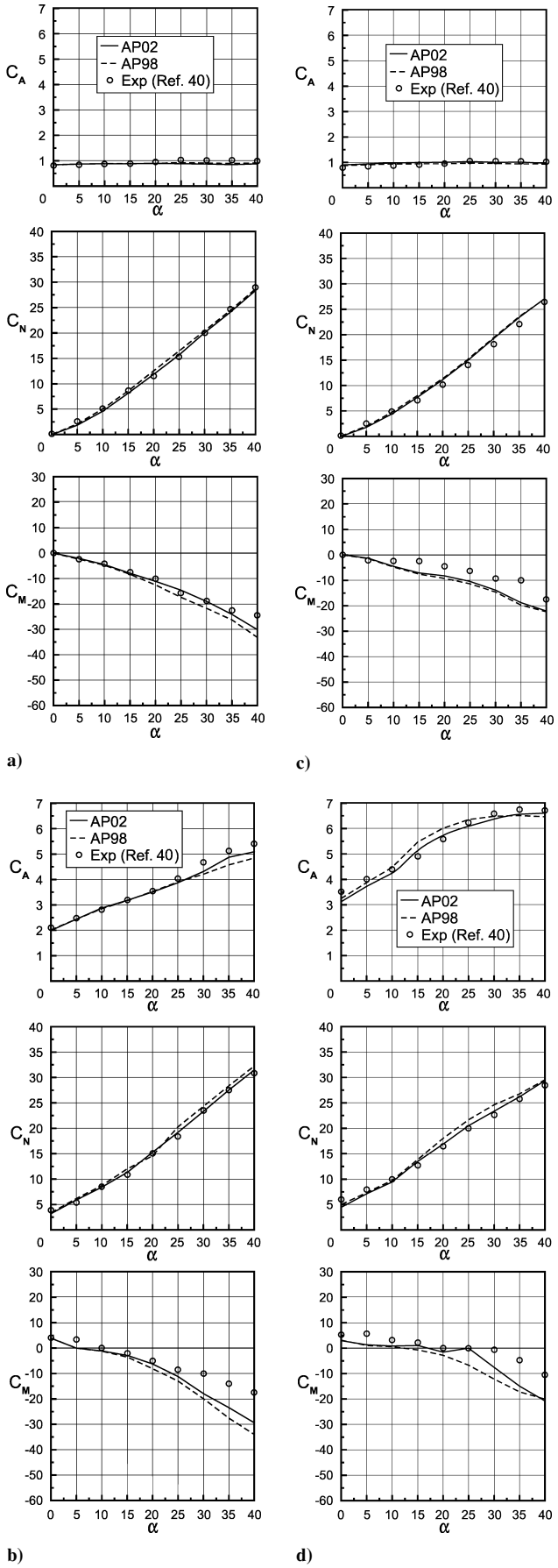

Fig. 4 Comparison of experiment and theory for C_A, C_N, and C_M for Fig 4 wing control case: a) M_∞ = 2.87, Φ = 0 deg, and δ_w = 0 deg; b) M_∞ = 2.87, Φ = 0 deg, and δ_w = 20 deg; c) M_∞ = 2.87, Φ = 45 deg, and δ_w = 0 deg; and d) M_∞ = 2.87, Φ = 45 deg, and δ_w = 20 deg.

The power-on base drag example is shown in Fig. 8 and is taken from Ref. 43. Two sets of experimental data are shown in Fig. 8, those of Refs. 43 and 44. The AP02 base pressure coefficient prediction compares fairly well with the Ref. 44 data at lower values of C_T and is in between the Ref. 43 and Ref. 44 data for higher values of C_T. The power-off base pressure coefficient is shown in Fig 8, illustrating that at very low values of thrust coefficient, power-on increases base drag, whereas for higher values of C_T, base drag is decreased. Figure 8 also illustrates one of the difficulties in assessing the accuracy of a prediction methodology when the values of the experimental measurements vary as much as shown in Fig. 8.

The next new technology that will be part of the AP02 is the trailing-edge flap capability. Again only one example case will be shown, and the data are taken from Ref. 35. The configuration tested is shown in Fig. 9. Figure 10 shows a comparison of theory and experiment for $(\Delta C_N)_f$ and $(\Delta C_M)_f$ at $\delta_f = -20$ deg and Mach number 2.96. Results are plotted as a function of AOA up to 30 deg. As seen in Fig. 10, the theory does a reasonable job in matching the data for both $(\Delta C_N)_f$ and $(\Delta C_M)_f$.

Also shown on the $(\Delta C_M)_f$ portion of Fig. 10 are the results from assuming the center of pressure of the flap is based on the flap in freestream flow as well as the flap attached to the trailing edge. The flap attached to the trailing edge computations take into account the center of pressure shift resulting from viscous effects.

Figure 11 shows a comparison of the theory and experiment for axial force coefficient where the trailing-edge flap has been deflected -10 and -30 deg, respectively. The equivalent value of

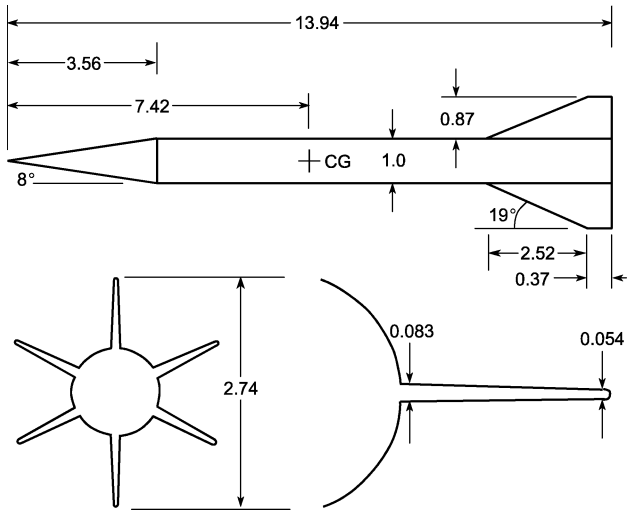

Fig. 5a Schematic of M735 projectile configuration (dimensions in calibers, where 1 caliber = 1.39 in.) (from Refs. 22 and 41).

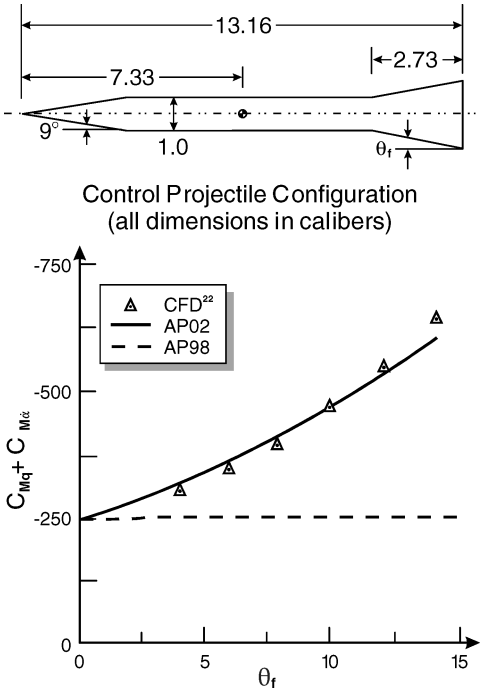

Fig. 6 Comparison of theoretical predictions of pitch damping moment coefficient for various flare angles (M_∞ = 4.4).

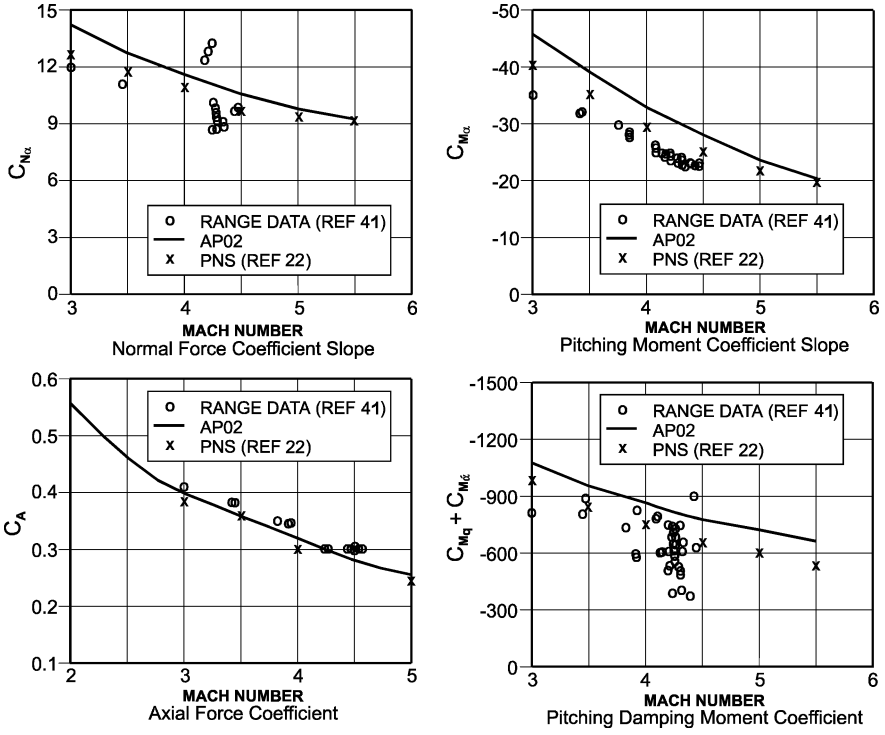

Fig. 5b Comparison of new multifin method with CFD and experiment for Fig. 6a configuration.

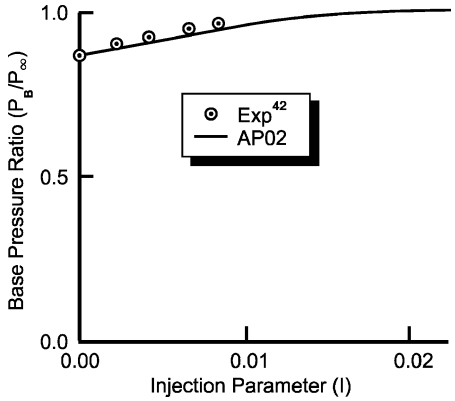

Fig. 7 Comparison of theory and experiment for base pressure ratio at base bleed conditions ($M_\infty = 0.98$, $d_j/d_r = 0.31$, and $t_j = 2150°$R).

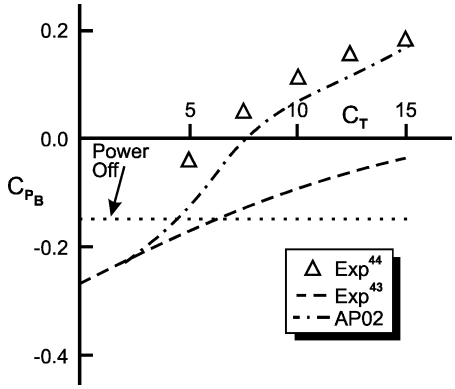

Fig. 8 Comparison of power-on-base pressure coefficient prediction with experiment ($M_j = 2.5$, $M_\infty = 1.94$, and $d_j/d_r = 0.75$).

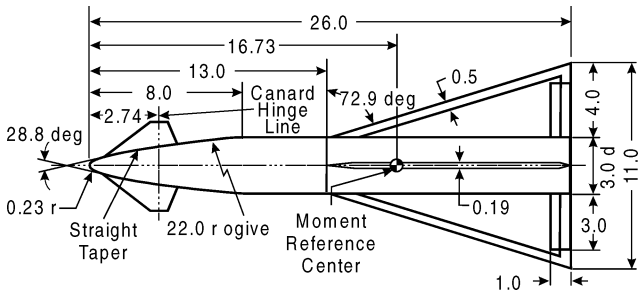

Fig. 9 Drawing of the model used for supersonic tests[35] (all linear dimensions in inches).

δ_W corresponding to $\delta_f = -10$ and -30 deg, respectively, is also shown in Fig. 11 as a function of freestream Mach number. Note that δ_W is only a small fraction of δ_f . The wing area is 8.67 times that of the trailing-edge flap. Two cases are shown for the theory: where the wind tunnel model has no boundary-layer trip and where the boundary-layer trip is present. The Reynolds number for the tests was 2.5×10^6. According to Ref. 35, a boundary-layer trip was present. Based on comparison of theory and experiment, it appears the boundary-layer trip was effective in producing a turbulent boundary layer over the surface at the lower supersonic Mach numbers. However, at the higher supersonic Mach numbers, it appears that the flow may partially transition back to laminar over much of the body and large wing for the $\delta = -10$ deg case. This relaminarization of the flow is speculated to be the reason the theory with no boundary-layer trip option agrees closer to the wind-tunnel data at high supersonic Mach number than does the theory which assumes turbulent flow over the entire surface of the model at all Mach numbers. If the preceding hypothesis of relaminarization of the flow is correct, the theory predicts the experimental data quite well. If this

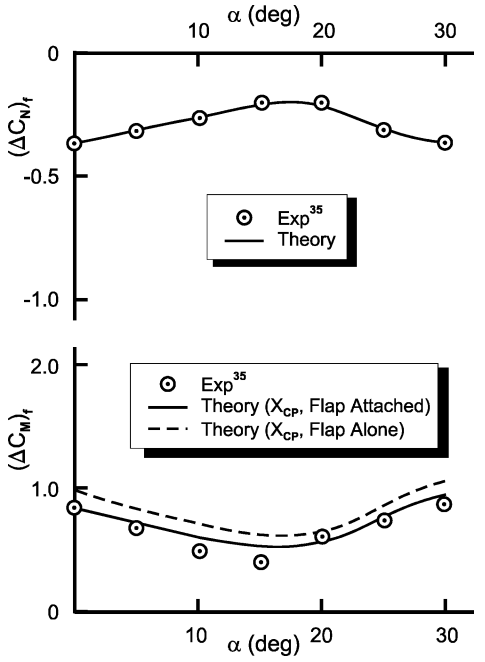

Fig. 10 Comparison of theory and experiment for normal-force and pitching moment coefficients of trailing-edge flaps ($M_\infty = 2.96$ and $\delta_f = -20$ deg).

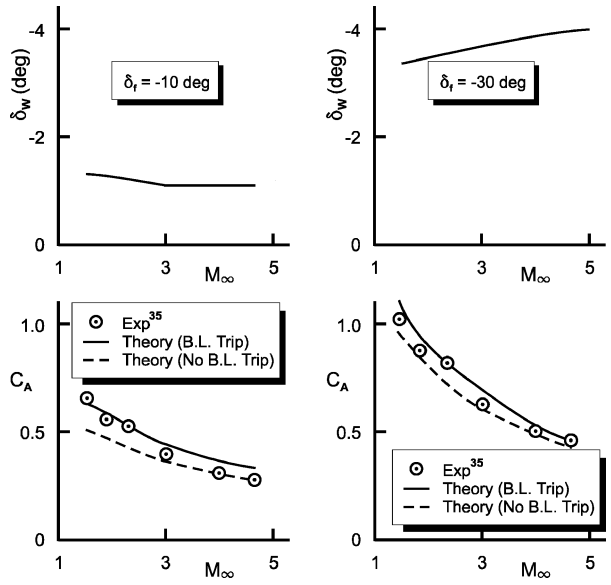

Fig. 11 Comparison of theory and experiment for axial-force coefficient at various values of flap deflection and as represented by an equivalent deflection of entire wing at $\alpha = 0$ deg (Re_N/ft = 2.5×10^6).

hypothesis is not correct, then the theory is high for Mach numbers 3.0 and greater.

The next example to illustrate the improvements in aerodynamic prediction that are encompassed in the AP02 is the improved axial force for nonaxisymmetric bodies. The case chosen is the square-body case from the ARF at Eglin Air Force Base.[14] The configuration tested is shown in Fig. 12. Hathaway et al.[14] tested all of the cases shown in Fig. 12, and Moore and Hymer[16] show additional comparisons of AP02 predictions to configurations other than the square for those interested. Figure 13 shows a comparison of the axial force coefficient of the AP02 with the modified axial force coefficient defined by Eq. (5) and the ARF data. Note that the modified AP02 results compare more favorably than the unmodified results, which are almost identical to the circular-body results. Figure 13 also shows the comparison of the normal-force

and pitching moment coefficient derivatives near alpha of 0 deg for the AP02 and ARF data along with the pitch damping moment. Note that the AP02 results are slightly different depending on the orientation of the square in flight, whereas the range data averages out these differences. In general, the AP02 gives good results for C_A and C_{N_α} and fair comparisons to the data for C_{M_α} and $C_{M_q} + C_{M_{\dot{\alpha}}}$.

The final illustration of the AP02 new methodology will show two examples utilizing the trajectory modules. The first example will illustrate the ballistic module specifically oriented to predicting range of spin-stabilized unguided ordnance.[37]

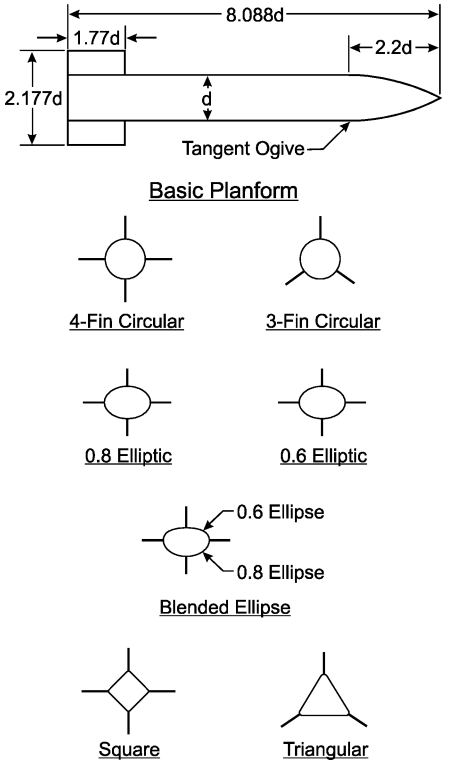

Fig. 12 Model cross section configuration tested at ARF.[14]

Figure 14a shows the configuration that will be considered for range computations. It is a 5-in.-diam round, 26 in. in length with a 3 caliber tangent ogive nose. The nose has a meplat diameter of 0.5 in., typical of most fuze designs. The round also has a 1-caliber boattail with a 7-deg boattail angle. The Fig. 14a configuration is assumed to weigh 65 lb and to have an initial velocity of 3000 ft/s. We will consider the range of this configuration when launched at an elevation angle of 50 deg. The free-flight boundary-layer option will be used for the aerodynamic computations because we are computing range.

Figure 14b shows the axial force coefficient vs Mach number for an AOA 1 deg. Figures 14c–14e show some of the many plots available in the AP02 interface. Figure 14c gives the altitude vs range, Fig. 14d provides the Mach number vs time of flight, and Fig. 14e gives the drag coefficient vs time of flight. Notice the round

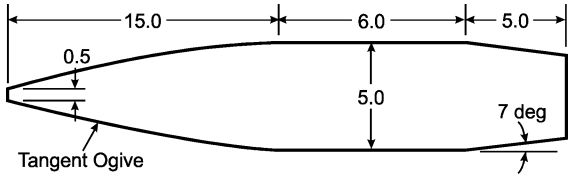

Fig. 14a Typical spin stabilization projectile (dimensions in inches).

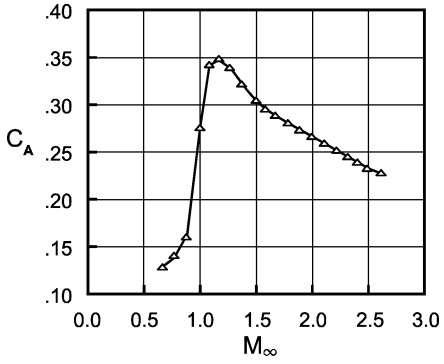

Fig. 14b Axial force coefficient vs Mach number for Fig. 14a configuration (α = 1 deg).

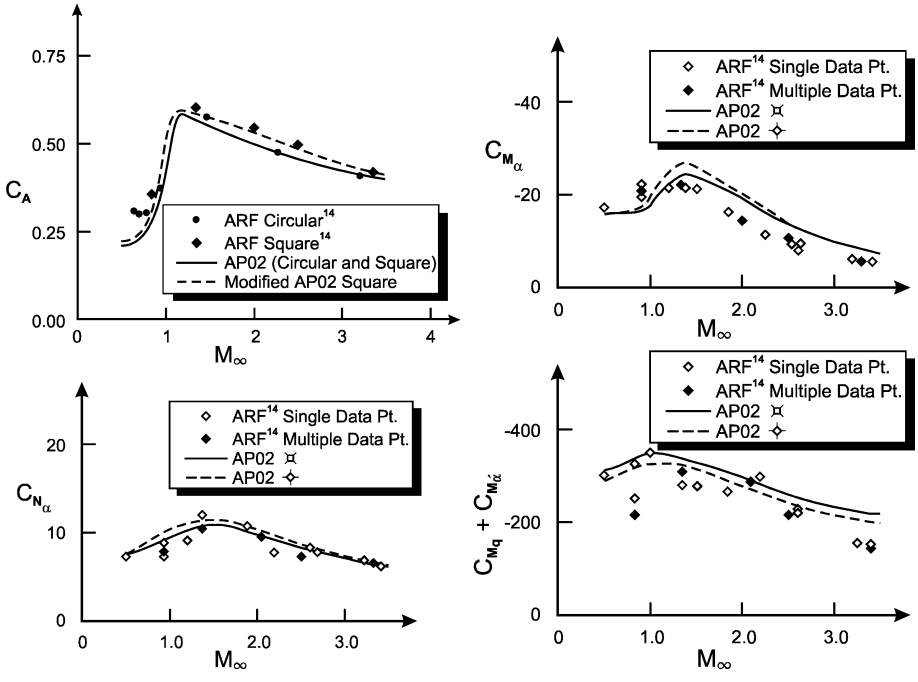

Fig. 13 Comparison of AP02 aerodynamic predictions to ARF range data.

Table 7 Parameters used in trajectory analysis for Fig. 16 configuration

600-lb Propellant		750-lb Propellant	
Parameter	Value	Parameter	Value
W_0	1500 lb	W_0	1500 lb
W_{BO}	900 lb	W_{BO}	750 lb
t_{BO}	10 s	t_{BO}	12.5 s
C.G.	5.5 ft at $t = 0$	C.G.	5.5 ft at $t = 0$
C.G.	5.0 ft at $t \geq 10$ s	C.G.	4.83 ft at $t \geq 12.5$ s
T_1	11,100 lb for 10 s	T_1	11,100 lb for 12.5 s
T_2	0 for $t > 10$ s	T_2	0 for $t > 12.5$ s
δ_{max}	± 30 deg	δ_{max}	± 30 deg
Gravitational acceleration limit	60 g	Gravitational acceleration limit	60 g
IV	100 ft/s	IV	100 ft/s
QE	45 deg	QE	45 deg

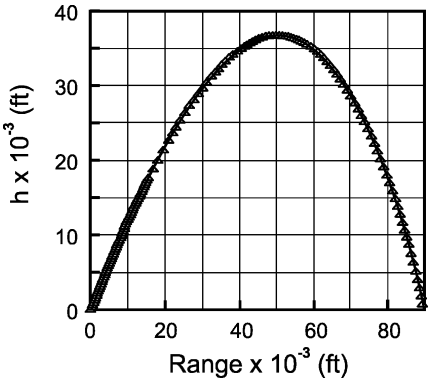

Fig. 14c Altitude vs range for Fig. 14a configuration (QE = 50 deg).

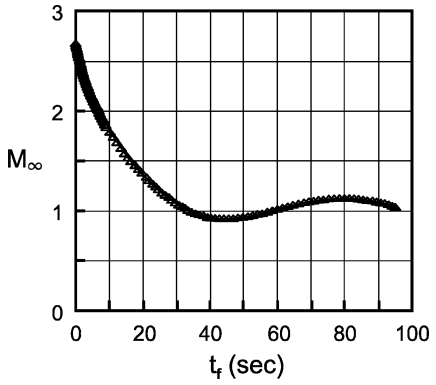

Fig. 14d Mach number vs time of flight for Fig. 14a configuration (QE = 50 deg).

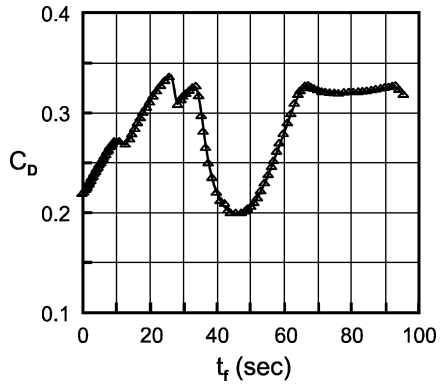

Fig. 14e Drag coefficient vs time of flight for Fig. 14a configuration (QE = 50 deg).

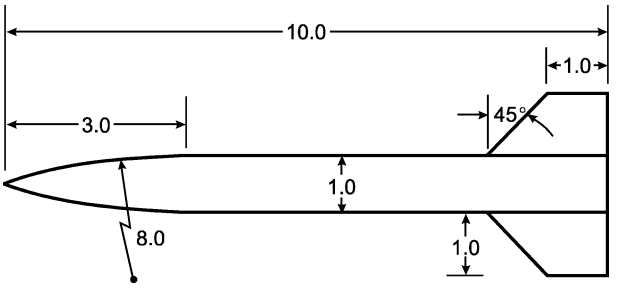

Fig. 15 Body–tail missile concept used in trajectory analysis (all dimensions in feet).

travels just under 90,000 ft (29,967 yards to be exact), with about 75% of the flight time between M_∞ of 1.2 and 0.9.

The second example to be illustrated using the new trajectory models uses the trim performance model. The configuration chosen is a simple body tail with a 3-caliber secant ogive (Fig. 15). The tail has an aspect ratio of 0.67. The parameters used in the trajectory analysis are provided in Table 7. The left-hand side (LHS) of Table 7 gives data for a configuration that has a 40% propellant to total weight ratio, whereas the right-hand side (RHS) is for a 50% propellant to total weight ratio. The initial thrust to weight ratio for both options in Table 7 is 7.4. The burn time is 10 s for the first configuration (LHS), whereas the second configuration (RHS) has a burn time of 12.5 s due to the 25% larger mass of propellant. Both configurations assume a maximum tail fin deflection of ± 30 deg, have a structural limit of 60 g, and are launched from a surface launcher with an exit velocity of 100 ft/s at an elevation angle of 45 deg. Figure 16 shows the results of flying the Fig. 15 configuration using the first configuration (LHS of Table 7) parameters in a purely ballistic mode. As seen in Fig. 16, a maximum Mach number of about 2.5 is obtained as the engine burns out after 10 s. The vehicle attains an altitude of about 20,000 ft and a range of about 100,000 ft using the set of conditions in Table 7 (LHS) and the drag curve provided internally within the AP02.

Figure 17 shows the very same conditions for Fig. 16, except a guidance mode is selected in the trim model that allows the vehicle to fly a maximum lift to drag ratio trajectory. For this case, the minimum Mach number is lower than shown in Fig. 16a due to the fin deflection and AOA. However, the altitude is slightly higher, and a range increase to 125,000 ft is realized due to the maximum L/D trajectory.

The final option is shown in Fig 18. This case is also for a maximum L/D trajectory, except the parameters of the RHS of Table 7 are used to fly the Fig. 15 configuration. Notice that a 25% increase in propellant produces a 40% increase in maximum Mach number (Fig. 18b compared to Fig. 17a) and a 45% increase in maximum range (Fig. 18b compared to Fig. 17b).

Figures 16–18 illustrate just one application of the trim performance model. One could examine variations in thrust, weight, c.g., or various other configuration design options very easily using the

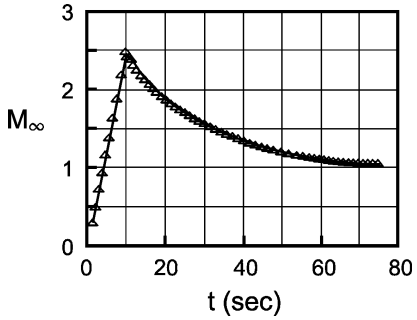

Fig. 16a Mach number profile for ballistic trajectory for Fig. 15 configuration with LHS of Table 7 parameters.

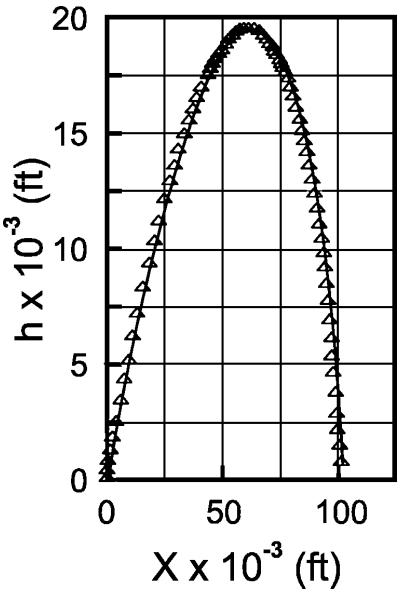

Fig. 16b Altitude vs range for ballistic trajectory for Fig. 15 configuration with LHS of Table 7 parameters.

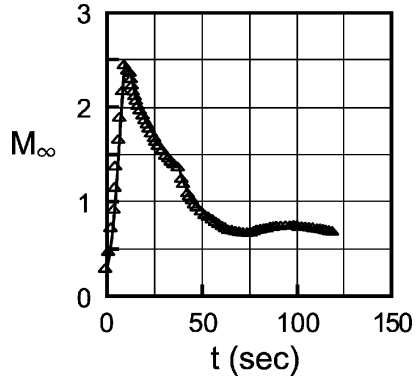

Fig. 17a Mach number profile for maximum *L*/*D* trajectory for Fig. 15 configuration with LHS of Table 7 parameters.

AP02 with a single person as opposed to the AP98 and all prior versions requiring two people. Other design options include various guidance modes including proportional navigation and explicit and a user-defined option as well. Initial launch conditions are allowed from a surface or air vehicle, and target parameters can be fairly general as well.

In summary, the new ballistic and trim performance models that will be part of the AP02 will allow the user to determine rapidly the effect of a given airframe or weapon system parameter on the overall performance of the vehicle. This new model will save many hours and many dollars through the provided productivity improvements.

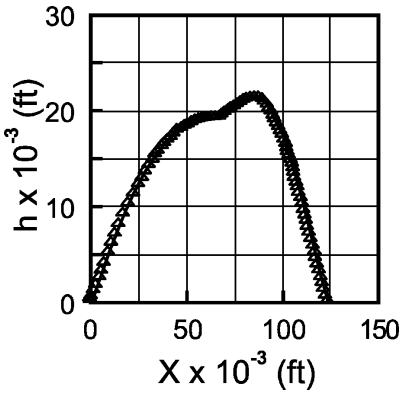

Fig. 17b Altitude vs range for maximum *L*/*D* trajectory for Fig. 15 configuration with LHS of Table 7 parameters.

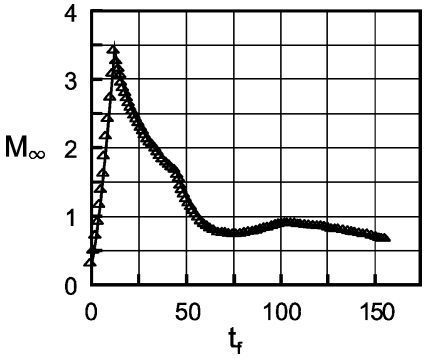

Fig. 18a Mach number profile for maximum *L*/*D* trajectory for Fig. 15 configuration with RHS of Table 7 parameters.

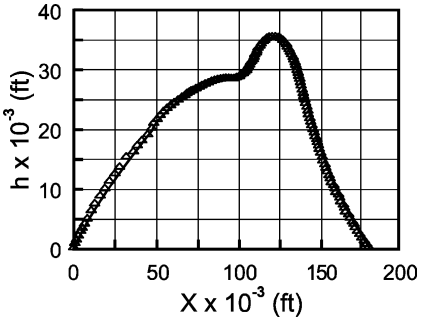

Fig. 18b Altitude vs range for maximum *L*/*D* trajectory for Fig. 15 configuration with RHS of Table 7 parameters.

Summary

In summary, new technology has been developed that will allow the APC to treat weapons in a more robust and accurate manner in the aerodynamic calculation process. Some of these new technologies include the capability to consider configurations with six and eight fins in addition to the present two- and four-fin options, improved nonlinear aerodynamics for higher AOA, improved dynamic derivatives with particular emphasis on pitch damping, improved power-on base drag prediction for rockets, a new base bleed capability for projectiles, improved axial force prediction of nonaxisymmetric bodies, and new technology that allows trailing-edge flap aerodynamics to be calculated. In addition to the new aerodynamics technology developed, several other improvements and productivity enhancements have been integrated into the APC. These include an aerodynamic smoother for the aerodynamics, ballistic and 3-DOF trajectory models, many additional plots in the postprocessor for APC output, and alternative reference length and area options in the pre-processor for the APC inputs. Many of the new technologies integrated into the AP98 that form the AP02 were driven by advanced projectile concepts.

When the new technology to predict the nonlinear aerodynamics was compared to both the AP98 and experimental data, it was seen that the AP02 reduces the average AP98 normal-force coefficient prediction errors by about 25%. Both the AP98 and AP02 give average normal-force and axial-force errors within the $\pm 10\%$ goal of the APC. Some slight improvement in axial-force, pitching moment, and center of pressure predictions were also seen using the AP02 but were not quantified.

In comparing the new multifin aerodynamic prediction capability of the AP02 and experimental data on a limited number of cases, it was seen that acceptable accuracy was obtained for static and dynamic aerodynamic coefficients. Additional multifin data would be desirable, particularly for eight-fin cases, to allow additional validation of the multifin capability.

The pitch damping improvements added to the APC code were seen to improve the pitch damping moment coefficient derivative accuracy compared to experiment for body alone and bodies with flares. Although not shown, the body-alone improvements will also improve the predictions of pitch damping for wing–body or body–tail cases as well.

The modified engine on base pressure prediction was seen to be as accurate or slightly more accurate than the AP98 predictions, while being much more robust in terms of input options. The new base bleed capability was seen to compare well to a range of experimental data for both cold and hot exhaust data.

Comparison of normal-force, pitching moment, and axial-force coefficients of the AP02 trailing-edge flap predictions to limited experimental data showed predictions to give acceptable accuracy. However, additional data for validation purposes would be desirable.

The aerodynamics of nonaxisymmetric bodies are seen to be slightly improved using the AP02 compared to the AP98. These improvements in aerodynamic prediction accuracy are due to the improvements added for axial-force coefficient and the improved nonlinear aerodynamics discussed earlier.

Finally, the ballistic and 3-DOF trajectory options available as part of the APC were seen to improve cost effectiveness of aerodynamic design, as well as performance assessment of conceptual design tradeoffs. The cost reductions were due to the single person vs two people with the AP98 being able to make design changes and examine the effect of the design changes on performance in a very rapid manner.

In general, it is believed the AP02 is by far the most robust, as well as the most accurate, of all prior versions of the APC. As such, the AP02 will be a significant capability for engineers in the conceptual and preliminary design phase of weapon development. The AP02 will also find use among personnel involved in numerical code calculations because the AP02 will approximate total aerodynamics one should expect from the numerical code.

Acknowledgments

The work described in this paper was partially supported by the Office of Naval Research (G. Graff) through the Surface Weapons Systems Technology Program managed at the Naval Surface Warfare Center, Dahlgren Division, by Robin Staton. Tasking from this program was provided by Roger Horman, John Fraysse, and Tim Spivak. George Long of the Standard Missile Program also provided some funding in past years. The work described in this paper was also partially supported by Aeroprediction 2002 sales.

References

[1]Moore, F. G., *Approximate Methods for Weapon Aerodynamics*, Vol. 186, Progress in Astronautics and Aeronautics, AIAA, Reston, VA, 2000.

[2]Moore, F. G., McInville, R. M., and Robinson, D. I., "A Simplified Method for Predicting Aerodynamics of Multi-Fin Weapons," U.S. Naval Surface Warfare Center, Rept. NSWCDD/TR-99/19, Dahlgren, VA, March 1999.

[3]Moore, F. G., McInville, R. M., and Robinson, D. I., "A Semiempirical Method for Predicting Multi-Fin Weapon Aerodynamics," AIAA Paper 2000-0766, Jan. 2000.

[4]Allen, J. M., "The Triservice Missile Data Base," NASA TM-2002-211653, June 2002.

[5]Allen, J. M., Hemsch, M. J., Burns, K. A., and Peters, K. J., "Parametric Fin–Body and Fin-Alone Data Base on a Series of 12 Missile Fins," NASA TM in publication, May 1996.

[6]Moore, F. G., and McInville, R. M., "Refinements in the Aeroprediction Code Based on Recent Wind Tunnel Data," U.S. Naval Surface Warfare Center, Rept. NSWCDD/TR-99/116, Dahlgren, VA, Dec. 1999.

[7]Moore, F. G., McInville, R. M., and Hymer, T. C., "Evaluation and Improvements to the Aeroprediction Code Based on Recent Test Data," *Journal of Spacecraft and Rockets*, Vol. 37, No. 6, 2000, pp. 720–730; also AIAA Paper 2000-4195, Aug. 2000.

[8]Moore, F. G., McInville, R. M., and Hymer, T. C., "Evaluation and Improvements to the Aeroprediction Code Based on Recent Test Data," *Journal of Spacecraft and Rockets*, Vol. 37, No. 6, 2000, pp. 720–730.

[9]Moore, F. G., and Hymer, T. C., "Improvement in Pitch Damping for the Aeroprediction Code with Particular Emphasis on Flare Configurations," U.S. Naval Surface Warfare Center, Rept. NSWCDD/TR-00/009, Dahlgren, VA, April 2000.

[10]Moore, F. G., and Hymer, T. C., "Semiempirical Prediction of Pitch Damping Moments for Configurations with Flares," *Journal of Spacecraft and Rockets*, Vol. 38, No. 2, 2001, pp. 150–158; also AIAA Paper 2001-0101, 2001.

[11]Moore, F. G., and Hymer, T. C., "Improved Power-On, Base Drag Methodology for the Aeroprediction Code," U.S. Naval Surface Warfare Center, Rept. NSWCDD/TR-00/67, Dahlgren, VA, May 2001.

[12]Moore, F. G., and Hymer, T. C., "Improved Semi-Empirical Method for Power-On Base-Drag Prediction," *Journal of Spacecraft and Rockets*, Vol. 39, No. 1, 2002, pp. 56–65; also AIAA Paper 2001-4328, Aug. 2001.

[13]Moore, F. G., McInville, R. M., and Hymer, T. C., "An Improved Semiempirical Method for Calculating Aerodynamics of Missiles with Noncircular Bodies," U.S. Naval Surface Warfare Center, Rept. NSWCDD/TR-97/20, Dahlgren, VA, Sept. 1997.

[14]Hathaway, W. H., Kruggel, B., Abate, G., Winchenbach, G., and Krieger, J., "Aeroballistic Range Tests of Missile Configurations with Noncircular Cross Sections," Munitions Directorate, U.S. Air Force Research Lab., Rept. AFRL-MN-EG-TR-2001-7082, Eglin AFB, FL, Sept. 2001.

[15]Moore, F. G., and Hymer, T. C., "A Semiempirical Method for Predicting Aerodynamics of Trailing Edge Flaps," U.S. Naval Surface Warfare Center, Rept. NSWCDD/TR-01/30, Dahlgren, VA, Oct. 2001.

[16]Moore, F. G., and Hymer, T. C., "The 2002 Version of the Aeroprediction Code: Part I–Summary of New Theoretical Methodology," U.S. Naval Surface Warfare Center, Rept. NSWCDD/TR-01/108, Dahlgren, VA, March 2002.

[17]Nielsen, J. N., *Missile Aerodynamics*, NEAR, Inc., Mountain View, CA, 1988.

[18]Stallings, R. L., Jr., and Lamb, M. L., "Wing-Alone Aerodynamic Characteristics for High Angles of Attack at Supersonic Speeds," NASA TP 1989, July 1981.

[19]Baker, W. B., Jr., "Static Aerodynamic Characteristics of a Series of Generalized Slender Bodies with and Without Fins at Mach Numbers from 0.6 to 3.0 and Angles of Attack from 0 to 180°," Arnold Engineering Development Center, Rept. TR-75-124, Vols. 1 and 2, Tullahoma, TN, May 1976.

[20]Pitts, W. C., Nielsen, J. N., and Kaatari, G. E., "Lift and Center of Pressure of Wing–Body–Tail Combinations at Subsonic, Transonic, and Supersonic Speeds," NACA TR 1307, 1957.

[21]Moore, F. G., McInville, R. M., and Hymer, T. C., "The 1998 Version of the NSWC Aeroprediction Code: Part I—Summary of New Theoretical Methodology," U.S. Naval Surface Warfare Center, Rept. NSWCDD/TR-98/1, Dahlgren, VA, April 1998.

[22]Sturek, W. B., Nietubicz, C. J., Sahu, J., and Weinacht, P., "Recent Applications of CFD to the Aerodynamics of Army Projectiles," U.S. Army Research Lab., Rept. ARL-TR-22, Aberdeen Proving Ground, MD, Dec. 1992.

[23]Weinacht, P., "Navier–Stokes Predictions of Pitch-Damping for a Family of Flared Projectiles," U.S. Army Research Lab., Rept. ARL-TR-591, Aberdeen Proving Ground, MD, Oct. 1994.

[24]Qin, N., Ludlow, D. K., Shaw, S. T., Edwards, J. A., and Dupuis, A., "Calculation of Pitch Damping Coefficients for Projectiles," AIAA Paper 97-0405, Jan. 1997.

[25]Weinacht, P., Sturek, W. B., and Schiff, L. B., "Navier–Stokes Predictions of Pitch-Damping for Axisymmetric Shell Using Steady Coning Motion," U.S. Army Research Lab., Rept. ARL-TR-575, Aberdeen Proving Ground, MD, Sept. 1994.

[26]Weinacht, P., "Prediction of Pitch-Damping of Projectiles at Low Supersonic and Transonic Velocities," AIAA Paper 98-0395, Jan. 1998.

[27]Wu, J. M., and Aoyoma, K., "Transonic Flow-Field Calculation Around Ogive Cylinders by Nonlinear–Linear Stretching Method," U.S. Army Missile Command, RD-TR-70-12, Redstone Arsenal, AL, April 1970; AIAA Paper 70-189, Jan. 1970.

[28]"Equations, Tables, and Charts for Compressible Flow," NACA Rept. 1135, 1953.

[29]Chin, S. S., *Missile Configuration Design*, McGraw–Hill, New York, 1961, pp. 134–138.

[30]Brazzel, C. E., and Henderson, J. H., "An Empirical Technique for Estimating Power-On Base Drag of Bodies-of-Revolution with a Single Jet Exhaust," AGARD Proceedings, Fluid Dynamics Panel, Sept. 1966.

[31]Danberg, J. E., "Analysis of the Flight Performance of the 155 mm M864 Base Burn Projectile," U.S. Army Research Lab., Rept. BRL-TR-3083, Aberdeen Proving Ground, MD, April 1990.

[32]Vukelich, S. R., and Jenkins, J. E., "Missile DATCOM: Aerodynamic Prediction on Conventional Missiles Using Component Build-Up Techniques," AIAA Paper 84-0388, 1984.

[33]"USAF Stability and Control DATCOM," Vols. 1 and 2, rev., Douglas Aircraft Co., Inc., Wright–Patterson AFB, OH, July 1963.

[34]Goin, K. L., "Equations and Charts for the Rapid Estimation of Hinge-Moment and Effectiveness Parameters for Trailing-Edge Controls Having Leading and Trailing Edges Swept Ahead of the Mach Lines," NACA TR 1041, 1951.

[35]Triscott, C. D., Jr., "Longitudinal Aerodynamic Characteristics at Mach 1.50 to 4.63 of a Missile Model Employing Various Canards and a Trailing-Edge Flap Control," NASA TM X-2367, Oct. 1971.

[36]Baldwin, A. W., and Adamczak, D. W., "Experimental Evaluation of Aerodynamic Control Devices for Control of Tailless Fighter Aircraft," Flight Dynamics Directorate, U.S. Air Force Research Lab., Rept. WL-TM-92-318, Wright–Patterson AFB, OH, April 1992.

[37]Hughes, S. V., and Jones, H. J., "A Point Mass Trajectory Model (TRAMOD) with Exterior Ballistic Analysis Enhancements," U.S. Naval Surface Warfare Center, Rept. NSWCDD/MP-98/41, Dahlgren, VA, April 1998.

[38]Phillips, C., "Standard Missile–2 (SM-2) Block IV Midcourse Engineering Model Formulation," U.S. Naval Surface Warfare Center, Rept. NSWC/TR-89/39, Dahlgren, VA, Feb. 1989.

[39]Hymer, T. C., and Moore, F. G., "Integration of the Aeroprediction Code with a Point Mass Ballistic Model (TRAMOD) with a Trim Three-Degree-of-Freedom Model (MEM)," U.S. Naval Surface Warfare Center, Rept. NSWCDD/TR-00/77, Dahlgren, VA, Aug. 2000.

[40]Monta, W. J., "Supersonic Aerodynamic Characteristics of a Sparrow III Type Missile Model with Wing Controls and Comparison With Existing Tail-Control Results," NASA TP 1078, Nov. 1977.

[41]Guidos, B. J., "Static Aerodynamics CFD Analysis for 120 MM Hypersonic KE Projectile Design," U.S. Army Research Lab., Rept. ARL-MR-84, Aberdeen Proving Ground, MD, Sept. 1984.

[42]Ding, Z., Liu, Y., and Chen, S., "A Study of Drag Reduction by Base Bleed at Subsonic Speeds," First International Symposium on Special Topics in Chemical Propulsion: Base Bleed, Athens, Nov. 1988.

[43]Martin, T. A., and Brazzel, C. E., "Investigation of the Effect of Low Thrust Levels on the Base Pressure of a Cylindrical Body at Supersonic Speeds," U.S. Army Missile Command, Rept. RD-TR-70-11, Redstone Arsenal, AL, May 1970.

[44]Henderson, J. H., "An Investigation for Modeling Jet Plume Effects on Missile Aerodynamics," U.S. Army Missile Command, Rept. TR RD-CR-82-25, Redstone Arsenal, AL, July 1982.

M. S. Miller
Associate Editor